11th WCRR World Congress on Railway Research 2016
29th May – 2nd June
Milan - Italy

Diagnostics Of Traction System Of Very High Speed trains: Experimental Results And Selection Of The Most Suitable Signal Processing Techniques

Paolo Pennacchi[1*], Steven Chatterton[1], Dimitrios Marinis[2], Antonio Didonato[2].

[1] Dipartimento di Meccanica, Politecnico di Milano, Via La Masa 1, I-20156, Milano, Italy.

[2] Bombardier Transportation, Via Tecnomasio 2, I-17047 Vado Ligure (SV), Italy

*Contact: paolo.pennacchi@polimi.it

Abstract

Traction equipment of very high speed trains (VHST) is characterized by high complexity and quality of the components and requires high reliability. An efficient maintenance approach like condition based maintenance (CBM) should be implemented to reduce the costs of preventive maintenance program. For this purpose, an experimental full scale test rig for the CBM of VHST traction equipment has been designed to investigate in detail, failures in the main mechanical components of system, i.e. motor, bearings and gearbox. The paper describes first the main characteristics of the testrig. Then, the results of a long test campaign is described in detail. Several damaged bearings, intentionally and artificially or owing to field use, have been installed (more than 60 configurations) and 12 different operating conditions, in terms of motor torque and speed, have been tested. Moreover, several signal processing techniques have been used, including the more traditional frequency and statistically based and the more sophisticated exploiting multi-domain and cyclostationarity approaches. Very positive results have been obtained and they prove, for the first time to best of authors' knowledge, that, by positioning suitably the sensor and by using an appropriate signal analysis technique, bearing defects can be identified, even under heavy environmental noise. The results allow defining: i) the most suitable sensor position and type to be installed for each component and ii) the most suitable technique for signal analysis in order to monitor the distinct signature of impending faults of the bearings, gearbox and motor.

1. Introduction

Very high speed trains (VHST) require powerful, small and light traction components. These have to operate reliably on various conditions and tracks (including cross-border operation), making the maintenance strategy crucial. Obviously, the simplest run-to-failure maintenance technique taking place only when a failure has occurred, must be avoided in the context of VHST operation. Nowadays the most commonly adopted approach is the time-based (or mileage) preventive maintenance, which sets a periodic interval to perform maintenance operations regardless of the health status of the physical asset. However, the high reliability required and the complex structure specific of rolling stock equipment make the cost of preventive maintenance higher than necessary, because components are maintained which might not need maintenance. Therefore, more efficient maintenance approaches, such as condition-based maintenance (CBM), should be implemented.

CBM is a maintenance program that recommends maintenance actions based on the assessment of the status of the components, performed analyzing signals coming from installed sensors. CBM attempts to avoid unnecessary maintenance tasks by taking actions only when there is evidence of abnormal behaviours of a physical asset, in this specific contest of the traction equipment, i.e. the electrical motor, the gearbox and the bearings.

In order to investigate the feasibility of a CBM approach on a VHST, actual traction components (traction motor fed by motor converter and traction gearbox), taken from a Bombardier high speed train application, have been tested on a special test-rig, built up with unique characteristics aimed to reproduce actual train operating conditions.

The CBM approach has been investigated thoroughly, focusing on the bearings of traction motor and traction gear. JRC test-rig, designed to develop specific CBM techniques for VHST, is aimed to reproduce accurately the environment and to consider the complete system instead of each single component (i.e. motor, inverter, gearbox, different kinds of bearings, etc.), reproducing also the actual relative movements of the motor, of the gearbox and of the wheel axle, caused by the wheel-track interaction, by employing specific moving platforms to which the components are connected. PoliMi's expected results about CBM of bearings were finding out which is the most suitable signals to be analysed and the most suitable technique among those already available for their analysis, in order to monitor the distinct signature of impending faults.

2. Description of JRC – CBM test-rig

The traction system installed on the test-rig has been taken from "REGINA" high speed train, manufactured by BOMBARDIER, able to reach a maximum speed of 250 km/h. It is composed of an electric motor, fastened, in real application, to the bogie by means of three elastic bushings, and of a gearbox, connected on the real train to the bogie by a reaction rod and to the wheel axle.

The traction motor is a converter driven 4-poles asynchronous motor, whose rotor is mounted on two different bearings: a single row, deep groove ball bearing (MP2) in the non-driven end side and a cylindrical roller bearing on the driven end side (MP1).

The gearbox follows the typical layout with a single reduction gear unit, with helical gearing. The helical pinion (input shaft) of the gearbox is connected to the electrical motor by a coupling capable to allow the relative movements between motor and gearbox. On the gearbox there are two tapered rolling bearings for the output shaft (BG3), that can be mounted directly on the wheel-set or on a hollow shaft fitted on the wheel-set, two cylindrical roller bearings (BG2), and one four contact point ball bearing for the input shaft (BG1). The split inner ring ball bearing supports the axial thrust of the input shaft.

Figure 1. Test-rig

The Traction System was tested by means of a dedicate Test-Rig. All traction equipment (motor and gear-box) were installed on a test bench in which the axle of the train is simulated by a dummy shaft and the train load is simulated by means of an electric brake motor. The vibrations coming from the tracks are emulated by vibrating platforms fixed to the traction components.

These platforms simulate the relative movement between the motor suspended on the bogie primary damper and the gearbox integral with the wheel axle. A moving platform supports the axle of the traction gearbox, by means of two bearings, and shakes it vertically replicating both the movement between the motor and gearbox and the shock and vibrations generated by the tracks. Another moving platform moves the traction motor in the two directions of the horizontal plane, replicating only the movement between the motor and gearbox. The gearbox axle is connected by means of a universal joint to an industrial parallel shaft gearbox, that is connected by means of a second universal joint to the brake motor. A torque meter is placed between the flanges connecting the first universal joint and the industrial gearbox, in order to measure the actual output torque of the traction equipment under test.

The measurement set-up on the gearbox includes: 4 dual accelerometers, measuring accelerations along X direction and temperature at each shaft end, 3 triaxial accelerometers, 2 placed in the proximity of the fast shaft end and one on the wheel shaft and 7 single-axis accelerometers: 4 measuring vertical accelerations at each shaft end, 3 measuring accelerations along Y axis on the thrust bearing of the fast shaft and on both sides of the wheel shaft.

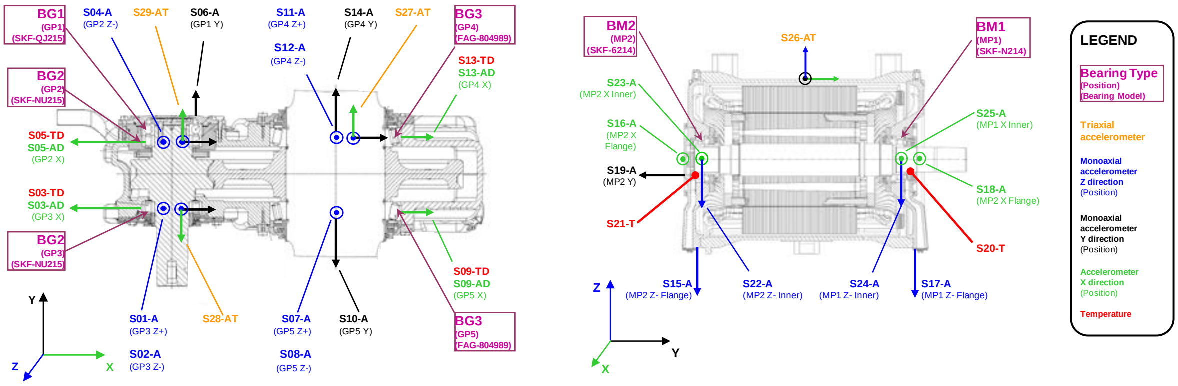

Figure 2. Location of sensors

The placement of single axis accelerometers and dual sensors has been studied to provide one temperature and two acceleration (Z-X) measurements for each bearing. An additional measurement, provided by single axis accelerometers, in y direction was set for the 3 bearings undergoing axial forces.

The choices for the measurement setup of the motor, have been driven by similar considerations and led to the following scheme: 5 single axis accelerometers measuring X and Y acceleration on the flanges of both the bearings an Y acceleration only on the ball bearing; 4 miniaturized single-axis accelerometers, placed in proximity of the bearings, in the inner part of the flange; 1 triaxial accelerometers, placed on top on the motor case; 2 thermistors, one per each bearing.

3. Damaged bearings

Figure 3. Examples of damage

During the campaign several damaged bearing have been tested. Different level of damages have been investigated, including electrical discharges, bad mounting, spalling, corrosion, oxidation in outer races, inner races and balls. Some examples of damage are shown in Figure 3.

4. Test campaign

The same test campaign of an overall duration of 140 minutes has been performed for each damaged bearing mounted on the test-rig. The schedule of a campaign consists in a warm-up of 15 minutes (at 160 km/h with 50% torque), followed by a series of 12 tests at different operating points. Between test 7 and 8 and between test 11 and 12, when the rotation direction is inverted, 2 cooling pauses of 10 minutes have been inserted. The different operating points have been chosen to provide examples of different conditions the train undergoes during normal operation (i.e. acceleration, braking, cruise). The vibration profiles executed by the platforms depend on the train speed the test-rig is simulating.

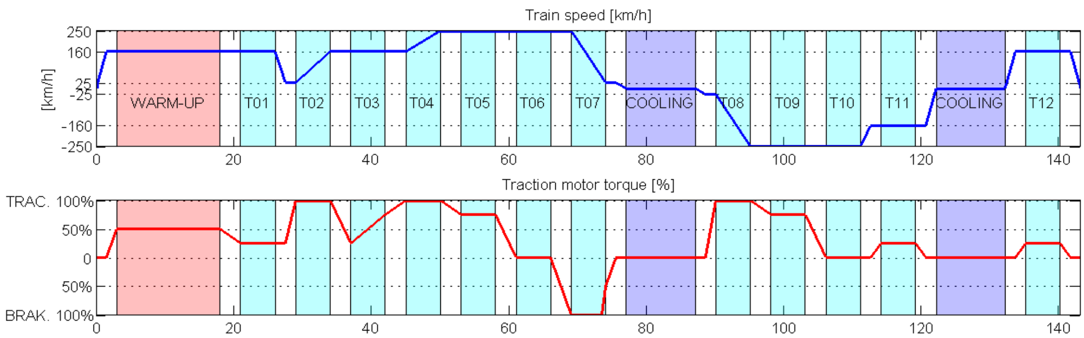

Figure 4. Speed and torque profiles of each campaign

5. Main results

Among the various analysis techniques proposed in literature, after a benchmark executed on the first campaigns, it has been pointed out how the most suitable ones for this particular application are Envelope

Analysis and Spectral Kurtosis. Both the techniques result in a spectrum-like indicator with, on the horizontal axis a range of frequencies, and on the vertical axis a technique-specific amplitude. A typical spectrum obtained by the Envelope Analysis of a damaged bearing is presented in Figure 5, from test campaigns with damaged BG1 (ball bearing on gearbox).

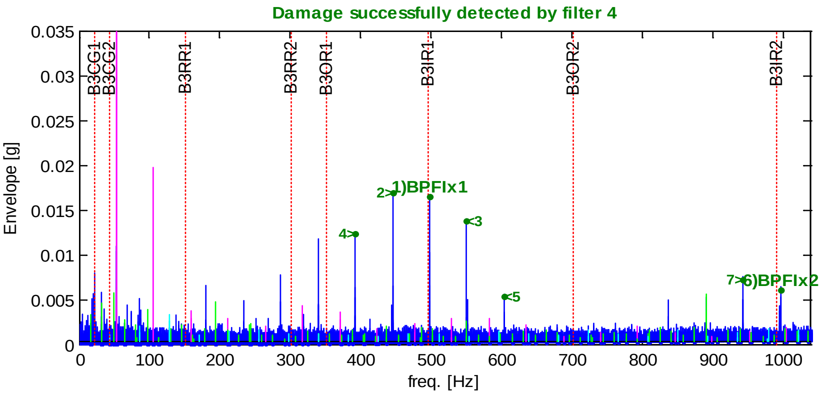

Figure 5. Example of Envelope Spectrum.

A damage, localized on a specific bearing component is evidenced by the appearance of peaks in the spectrum-like indicator at frequencies close to the nominal defect frequencies of the bearing. For each bearing is possible, knowing its geometrical dimensions to calculate the characteristic frequencies given a specific shaft rotating speeds and then check for correspondences in the indicator.

All the results by using Envelope Analysis are shown in Figure 6, where the percentage of sensors successfully detecting the damage is reported in each cell for all operating conditions (columns) and all bearing configurations (rows).

Percentage of sensors successfully detecting the damage		TST												
		1	*2*	**3**	*4*	**5**	**6**	*7*	*8*	**9**	**10**	**11**	**12**	
FILE	CFG	EN	*EN*	EN	*EN*	EN	EN	*EN*	*EN*	EN	EN	EN	EN	
	00													REF
TST-02.xlsm	02	100%	*0%*	92%	*0%*	100%	0%	*0%*	*0%*	8%	0%	42%	92%	GRB
TST-03.xlsm	03	100%	*0%*	100%	*0%*	50%	8%	*0%*	*0%*	25%	0%	42%	100%	
TST-04.xlsm	04	83%	*0%*	83%	*0%*	8%	67%	*0%*	*0%*	8%	8%	0%	50%	
TST-05.xlsm	05	67%	*0%*	33%	*0%*	75%	17%	*0%*	*0%*	0%	0%	33%	50%	
TST-06.xlsm	06	58%	*0%*	100%	*0%*	75%	0%	*0%*	*0%*	8%	8%	83%	42%	
TST-07.xlsm	07	0%	*0%*	0%	*0%*	8%	0%	*0%*	*0%*	0%	0%	8%	0%	
TST-08.xlsm	08	100%	*0%*	75%	*0%*	92%	0%	*0%*	*0%*	92%	0%	100%	83%	
	09													REF
TST-10.xlsm	10	17%	*0%*	25%	*0%*	33%	17%	*0%*	*0%*	0%	0%	0%	8%	GRB
TST-11.xlsm	11	8%	*0%*	8%	*0%*	8%	8%	*0%*	*0%*	8%	0%	0%	17%	
TST-12.xlsm	12	8%	*0%*	33%	*0%*	75%	0%	*0%*	*0%*	0%	0%	0%	0%	
TST-13.xlsm	13	83%	*0%*	75%	*0%*	100%	17%	*0%*	*0%*	17%	0%	8%	50%	
TST-14.xlsm	14	27%	*0%*	0%	*0%*	0%	91%	*0%*	*0%*	0%	0%	0%	0%	
TST-15.xlsm	15	100%	*0%*	100%	*9%*	100%	9%	*0%*	*0%*	100%	0%	9%	100%	
TST-16.xlsm	16	91%	*0%*	100%	*0%*	82%	55%	*0%*	*0%*	0%	9%	0%	0%	
TST-17.xlsm	17	82%	*0%*	64%	*0%*	73%	9%	*0%*	*0%*	55%	0%	55%	27%	
	18													REF
TST-19.xlsm	19	0%	*0%*	8%	*8%*	8%	58%	*0%*	*0%*	83%	67%	58%	58%	MOT (Real Field)
TST-20.xlsm	20	42%	*0%*	33%	*0%*	83%	50%	*0%*	*0%*	100%	92%	50%	50%	
TST-21.xlsm	21	0%	*0%*	0%	*0%*	33%	33%	*0%*	*0%*	67%	33%	42%	50%	
TST-22.xlsm	22	8%	*0%*	8%	*0%*	8%	33%	*0%*	*0%*	67%	42%	50%	25%	
	23													REF
TST-24.xlsm	24	43%	*0%*	14%	*0%*	0%	14%	*0%*	*0%*	86%	57%	86%	57%	MOT
TST-25.xlsm	25	0%	*0%*	14%	*0%*	29%	29%	*0%*	*0%*	71%	14%	14%	71%	
TST-26.xlsm	26	0%	*0%*	0%	*0%*	0%	0%	*0%*	*0%*	71%	14%	86%	43%	
TST-27.xlsm	27	86%	*0%*	29%	*29%*	0%	0%	*0%*	*0%*	86%	14%	100%	71%	
TST-28.xlsm	28	14%	*0%*	14%	*0%*	29%	0%	*0%*	*0%*	71%	43%	43%	100%	
TST-29.xlsm	29	14%	*0%*	0%	*0%*	29%	29%	*0%*	*0%*	43%	14%	14%	100%	
TST-30.xlsm	30	57%	*0%*	29%	*0%*	0%	0%	*0%*	*0%*	71%	14%	86%	14%	
TST-31.xlsm	31	0%	*0%*	0%	*0%*	14%	0%	*0%*	*0%*	86%	29%	43%	0%	
TST-32.xlsm	32	86%	*0%*	57%	*0%*	0%	0%	*0%*	*0%*	29%	57%	0%	29%	
TST-33.xlsm	33	43%	*0%*	71%	*57%*	57%	86%	*0%*	*0%*	100%	100%	57%	71%	
TST-34.xlsm	34	0%	*0%*	14%	*0%*	29%	29%	*0%*	*0%*	29%	29%	29%	71%	
TST-35.xlsm	35	29%	*0%*	29%	*0%*	29%	100%	*0%*	*0%*	71%	57%	71%	100%	
TST-36.xlsm	36	75%	*0%*	0%	*0%*	75%	13%	*0%*	*0%*	100%	50%	75%	88%	
TST-37.xlsm	37	38%	*0%*	0%	*0%*	100%	13%	*0%*	*0%*	100%	0%	100%	75%	
TST-38.xlsm	38	75%	*0%*	38%	*0%*	100%	100%	*0%*	*0%*	100%	100%	100%	75%	
TST-39.xlsm	39	13%	*0%*	0%	*0%*	100%	63%	*0%*	*0%*	100%	100%	100%	25%	

Figure 6. Successful recognitions for each damaged bearing (rows) and operating condition (columns).

For the high speed shaft of the gearbox (bearing configurations from 02 to 17), it is evident that best results, for all damaged bearing configurations, were obtained in the first 6 operating points, where torque-originated vertical load on the fast shaft bearings is added to the weight of the shaft itself. On the contrary, in the tests 9 to 11, the torque, whose direction has been switched, generates a load in the opposite direction of shaft weight, counterbalancing its effect and unloading the damaged bearing. In these operating conditions, as expected, recognition was more difficult because of the low energy involved in the damage-related impacts. The differences in recognition capability between operating conditions 1 and 12, that presents the same profile of torque and speed, is probably due to the increase in temperature and, consequently in lubricant fluidity. Better lubrication conditions would in fact lead to lower stresses in the discontinuity generated by the damage, resulting in a more difficult identification. For the motor bearings the best results, for all damaged bearing configurations (from 19 to 39), were obtained in the last 4 operating points. The differences in recognition capability are probably due again to lubrication issues. However, on the contrary of the gearbox case, since lubricant is grease, the higher temperature and the long run makes possible for the damage to be cleaned from grease, while at the beginning of the campaign the lubricant was masking the defect.

Conclusions

By means of the test rig described in the paper and equipped with high power traction components it has been possible to identify the condition of the bearings installed, in a scientific and structured manner. The positive results obtained with several bearing damages, confirmed the possibility to develop a CBM strategy for the maintenance of traction systems on VHST.
The research activity provided several insights on the features that a CBM algorithm should have for this specific application. Envelope Analysis, implemented on two different hardware and software systems, and Spectral Kurtosis have been chosen as the most effective and robust techniques, both at constant speed and in slow transients, such as the ones characterizing rail application.

References

1. Ferreira, J.L.A., Balthazar, J.C. and Araujo, A.P.N., An investigation of rail bearing reliability under real conditions of use, *Engineering Failure Analysis*, Vol. **10**, No. 6 (2003), pp. 745-758.
2. Randall, R.B., Antoni, J. and Chobsaard, S., The relationship between spectral correlation and envelope analysis in the diagnostics of bearing faults and other cyclostationary machine signals, *Mechanical Systems and Signal Processing*, Vol. **15**, No. 5 (2001), pp. 945-962.
3. Harvey, T.J., Wood, R.J.K. and Powrie, H.E.G., Electrostatic wear monitoring of rolling element bearings, *Wear*, Vol. **263**, No. 7-12 (2007), pp. 1492-1501.
4. Manoj, V., Manohar Shenoy, K. and Gopinath, K., Developmental studies on rolling contact fatigue test rig, *Wear*, Vol. **264**, No. 7-8 (2008), pp. 708-718.
5. Choy, F.K., Zhou, J., Braun, M.J. and Wang, L., Vibration monitoring and damage quantification of faulty ball bearings, *Journal of Tribology*, Vol. **127**, No. 4 (2005), pp. 776-783.
6. Hao, R. and Chu F., Morphological undecimated wavelet decomposition for fault diagnostics of rolling element bearings, *Journal of Sound and Vibration*, Vol. **320**, No. 4-5 (2009), pp. 1164-1177
7. Wang, W.Q., Ismail, F. and Golnaraghi, M.F., Assessment of gear damage monitoring techniques using vibration measurements, *Mechanical Systems and Signal Processing*, Vol. **15**, No. 5 (2001), pp. 905-922.
8. Oztürk, H., Sabuncu, M. and Yesilyurt, I., Early detection of pitting damage in gears using mean frequency of scalogram, *Journal of Vibration and Control*, Vol. **14**, No. 4 (2008), pp. 469-484.
9. Wang, W., Early detection of gear tooth cracking using the resonance demodulation technique, *Mechanical Systems and Signal Processing*, Vol. **15**, No. 5 (2001), pp. 887-903.
10. Sawalhi, N. and Randall, R.B., Simulating gear and bearing interactions in the presence of faults: Part I. The combined gear bearing dynamic model and the simulation of localised bearing faults, *Mechanical Systems and Signal Processing*, Vol. **22**, No. 8 (2008), pp. 1924-1951.
11. P. Pennacchi, S. Bruni, S. Chatterton, R. Ricci, P. Borghesani, F. Gherardi, D. Marinis, A. Didonato, F. Unger-Weber, Design Of A Test-Rig For Traction Equipment Of Very High Speed Trains, Proceedings of the 8th IFToMM International Conference on Rotordynamics, September 12-15, 2010, KIST, Seoul, Korea.